Research Square

Preprints are preliminary reports that have not undergone peer review.
They should not be considered conclusive, used to inform clinical practice,
or referenced by the media as validated information.

Pasteurization-assisted solid-state bioconversion of *Caragana korshinskii* residues by *Irpex lacteus* n6

xueying Liu
Inner Mongolia Agricultural University
liqiong Yan
liqiongyan@imau.edu.cn
Inner Mongolia Agricultural University https://orcid.org/0009-0002-1006-9629
liyan Zhang
Inner Mongolia Agricultural University
yaoran Zhang
Inner Mongolia Agricultural University
junhan Weng
Inner Mongolia Agricultural University
yue Bai
Inner Mongolia Agricultural University
yanhong He
Inner Mongolia Agricultural University

Research Article

Keywords: Caragana korshinskii, Irpex lacteus, fungal screening, pasteurization, solid-state fermentation, lignocellulosic bioconversion

Posted Date: October 12th, 2026

DOI: https://doi.org/10.21203/rs.3.rs-11126330/v1

License: This work is licensed under a Creative Commons Attribution 4.0 International License.
Read Full License

Abstract

The utilization of *Caragana korshinskii* residues as forage is constrained by their lignified structure and limited digestibility. In this study, eleven wild *Irpex lacteus* isolates collected from *C. korshinskii* habitats in western Inner Mongolia were screened for substrate colonization and lignocellulose-degrading potential. All isolates colonized shredded *C. korshinskii* residue medium, while isolates n4 and n6 reached the maximum measurable colony diameter of 70.00 mm after 7 d. Guaiacol, aniline blue, and carboxymethyl cellulose-Congo red assays revealed isolate-dependent differences in oxidative and cellulolytic responses. Among four isolates selected for quantitative enzyme analysis, isolate n6 exhibited the highest laccase, lignin peroxidase, and manganese peroxidase activities, reaching 3.59, 11.33, and 9.30 U mL^{-1}, respectively, together with the highest filter paper activity; its *β*-glucosidase activity was also among the highest measured. Orthogonal screening and validation identified maltose, peptone, initial pH of 4.5, and 30°C as suitable conditions for mycelial growth. Among the five grain substrates tested, buckwheat supported the most rapid inoculum propagation. After 56 d of solid-state fermentation, inoculation with *I. lacteus* n6 following pasteurization reduced the measured concentrations of neutral detergent fiber, acid detergent fiber, and acid detergent lignin by 16.78%, 16.54%, and 49.19%, respectively, relative to the corresponding uninoculated control. The measured crude protein and water-soluble carbohydrate concentrations increased from 8.18% to 12.10% and from 0.99% to 5.53%, respectively. These findings demonstrate the potential of a locally derived *I. lacteus* isolate for pasteurization-assisted solid-state bioconversion of *C. korshinskii* residues and provide a basis for their forage-oriented valorization.

1. Introduction

The increasing demand for animal protein and the resulting pressure on conventional feed resources have strengthened the need to develop alternative feedstocks for sustainable livestock production (Makkar, 2018). *Caragana korshinskii* Kom., a drought- and cold-tolerant leguminous shrub widely planted in the arid and semi-arid regions of northern China, is an important species in the Three-North Shelterbelt Program (Mei et al., 2025). Its extensive root system and resistance to wind erosion contribute to sand fixation, vegetation restoration, and the recovery of fragile ecosystems (Yu et al., 2026). As *C. korshinskii* shrublands mature, their productivity and structural condition may decline, and stubble cutting is commonly used to stimulate vegetative regeneration and restore stand vitality (Fang et al., 2008; Ma et al., 2026). More than 4 million tonnes of *C. korshinskii* pruning residues are produced annually in China, yet most of this material is burned or used as low-value fuel and remains underutilized. These residues therefore represent a large, readily available potential feedstock for animal feed, bio-based chemicals, and biomaterials. Their direct use as forage, however, is restricted by the progressive lignification of mature tissues, which reduces palatability and limits the accessibility of structural carbohydrates (Ju et al., 2023; Li et al., 2021).

Biological processing, including ensiling and fungal solid-state fermentation (SSF), offers a potentially mild route for upgrading lignocellulosic residues. Ensiling with *Lactiplantibacillus plantarum* can improve

fermentation quality and suppress undesirable microorganisms, but its ability to disrupt the lignin–carbohydrate matrix is limited (Zhou et al., 2025). White-rot fungi provide a complementary approach because they secrete extracellular oxidative and hydrolytic enzymes capable of modifying lignified plant cell walls. Fungal treatment has been associated with reductions in lignin-related barriers and phenolic compounds in agricultural residues, thereby increasing the accessibility of cell-wall carbohydrates (Zhang et al., 2023). In addition, fungal biomass may contribute to the measured crude protein concentration of the treated substrate. Nevertheless, conventional fungal SSF commonly uses steam sterilization or autoclaving, which increases energy consumption and may limit process scalability. A practical process for *C. korshinskii* bioconversion should therefore combine effective fungal colonization and lignocellulose modification with a lower-severity pretreatment.

Among white-rot fungi, *Irpex lacteus* has attracted attention because of its ligninolytic enzyme system, broad substrate adaptability, and ability to modify diverse straw-based feedstocks (Novotný et al., 2009; Qin et al., 2018; Wang et al., 2024). Its colonization and degradation performance, however, are strongly influenced by substrate structure, lignin composition, moisture, and other physicochemical properties (Rouches et al., 2016). Results obtained with wheat straw and other annual crop residues cannot therefore be directly extrapolated to shrub-derived biomass. In particular, it remains unclear whether *I. lacteus* isolates originating from arid and semi-arid *C. korshinskii* habitats possess phenotypic traits that support efficient colonization and lignocellulose modification of this locally abundant substrate. Furthermore, whether pasteurization can provide a practical alternative to autoclaving for *I. lacteus*-based SSF of *C. korshinskii* residues requires systematic evaluation.

In this study, eleven wild *I. lacteus* isolates obtained from representative *C. korshinskii* stands in western Inner Mongolia were evaluated through a stepwise screening strategy. The isolates were compared in terms of vegetative compatibility, growth on shredded *C. korshinskii* residue medium, and qualitative lignocellulolytic responses in guaiacol, aniline blue, and CMC-Congo red assays. Selected isolates were subsequently assessed for ligninolytic and cellulolytic enzyme activities, and isolate n6 was selected for further process development. Single-factor experiments, orthogonal screening, and validation experiments were conducted to identify suitable culture conditions, while grain-based substrates were assessed for inoculum propagation. Finally, the effects of pasteurization and autoclaving on the chemical composition of *C. korshinskii* residues during n6-inoculated SSF were compared. This study aimed to identify a locally derived *I. lacteus* isolate with strong lignocellulose-degrading potential, establish suitable conditions for its propagation, and evaluate changes in the fiber and nutrient composition of *C. korshinskii* residues following pasteurization-assisted SSF.

2. Materials and methods

2.1 Fungal strains and vegetative incompatibility assay

Eleven *I. lacteus* isolates (n1-n11) were obtained from the fungal culture collection of the College of Forestry, Inner Mongolia Agricultural University. The isolates were originally recovered from dead

branches of *C. korshinskii* collected at different locations in Inner Mongolia, China (Table 1). Before use, the isolates were revived on potato dextrose agar (PDA) at 25°C and maintained on PDA slants at 4°C.

Table 1
Geographic origins of the *I. lacteus* isolates used in this study

Isolate	Origin	Sampling coordinates (N, E)
n1	Helinger County, Hohhot	40.18°N, 111.77°E
n2	Siziwang Banner, Ulanqab	42.04°N, 111.54°E
n3	Qingshuihe County, Hohhot	39.76°N, 111.72°E
n4	Togtoh County, Hohhot	40.25°N, 111.38°E
n5	Hangjin Banner, Ordos	40.14°N, 107.77°E
n6	Darhan Muminggan United Banner, Baotou	41.43°N, 110.54°E
n7	Guyang County, Baotou	41.25°N, 110.21°E
n8	Jungar Banner, Ordos	39.88°N, 111.23°E
n9	Otog Banner, Ordos	39.27°N, 108.04°E
n10	Uxin Banner, Ordos	38.74°N, 109.11°E
n11	Dalad Banner, Ordos	40.49°N, 109.15°E

Vegetative compatibility was assessed by pairwise confrontation. Mycelial plugs (7 mm in diameter) were excised from the margins of actively growing colonies and placed on opposite sides of PDA plates. Plates were incubated at 25°C until the colonies met and interaction boundaries developed. Distinct demarcation or barrage lines at the colony interface were recorded as vegetative incompatibility reactions. Each of the 55 unique inter-isolate pairings was tested on three independent replicate plates.

2.2 Primary screening of lignocellulose-degrading isolates

The ability of the eleven isolates to colonize *C. korshinskii* was evaluated on shredded residue medium, and colony diameter was monitored for 7 d. Ligninolytic and cellulolytic potential was assessed using chromogenic plate assays. Oxidative activity was screened on PDA supplemented with guaiacol (0.04%, v/v) or aniline blue (0.01%, w/v), whereas cellulolytic activity was screened on PDA containing carboxymethyl cellulose (CMC; 0.5%, w/v) and Congo red (0.02%, w/v) (Teather and Wood, 1982; Liu et al., 2018; Li et al., 2020). Mycelial plugs (7 mm in diameter) were inoculated onto the corresponding media and incubated at 25°C for 5 d. Colony diameter (R) and the diameter of the coloration, decolorization, or hydrolysis zone (r) were measured, and the R/r ratio was calculated as a semiquantitative indicator of enzymatic potential.

2.3 Quantitative assessment of lignocellulose-degrading enzyme activities

2.3.1 Crude enzyme extraction

Following primary screening, isolates n1, n6, n8, and n9 were cultivated on shredded *C. korshinskii* residue medium for 10 d. A crude extracellular enzyme extract was prepared by mixing 2.0 g of fermented substrate with 20.0 mL of 50 mM sodium acetate buffer (pH 5.0) at a solid-to-liquid ratio of 1:10 (w/v). The mixture was incubated at 4°C for 30 min with orbital shaking at 180 rpm, then centrifuged at 8000 × g for 15 min at 4°C. The supernatant was collected as the crude enzyme extract and stored at 4°C until analysis.

2.3.2 Manganese peroxidase (MnP) activity

MnP activity was determined based on the H_2O_2-dependent formation, with minor modifications to the method of Wariishi et al. (1992). The 4.0 mL reaction system contained 2.5 mL of 50 mM sodium succinate buffer (pH 4.5), 0.4 mL of 1.6 mM $MnSO_4$, 1.0 mL of diluted crude enzyme, and 0.1 mL of freshly prepared 10 mM H_2O_2. Reactions were initiated by H_2O_2 addition and incubated at 37°C for 3 min; absorbance was measured at 270 nm.

2.3.3 Lignin peroxidase (LiP) activity

LiP activity was determined based on the H_2O_2-dependent oxidation of veratryl alcohol to veratraldehyde (Tien and Kirk, 1988), with minor modifications. The 1.0 mL reaction mixture consisted of 50 mM sodium tartrate buffer (pH 3.0), 2.0 mM veratryl alcohol, 0.4 mM freshly prepared H_2O_2, and 0.1 mL of diluted crude enzyme. After incubation at 30°C for 5 min, absorbance was recorded at 310 nm.

2.3.4 Laccase activity

Laccase activity was measured using 2,2'-azino-bis (3-ethylbenzothiazoline-6-sulfonic acid) (ABTS) as the substrate. The 3.0 mL reaction system contained 2.7 mL of 50 mM sodium acetate buffer (pH 4.5), 0.2 mL of 10 mM ABTS, and 0.1 mL of diluted crude enzyme. Absorbance was recorded at 420 nm after incubation at 30°C for 5 min.

2.3.5 Endoglucanase activity

Endoglucanase activity was determined using yl cellulose (CMC) as substrate, with reducing sugar release quantified by the 3,5-dinitrosalicylic acid (DNS) method (Miller, 1959; Ghose, 1987). The 1.0 mL reaction system contained 0.5 mL of diluted crude enzyme and 0.5 mL of 2% (w/v) CMC dissolved in 50 mM sodium citrate buffer (pH 4.8), giving a final CMC concentration of 1% (w/v). After incubation at 50°C for 30 min, the reaction was terminated by adding 3.0 mL of DNS reagent, followed by boiling for 5 min. After cooling to room temperature, absorbance was measured at 540 nm. Reducing sugar concentration was calculated against a D-glucose calibration curve processed under identical conditions.

2.3.6 Exoglucanase activity

Exoglucanase activity was assayed using 1% (w/v) microcrystalline cellulose (Avicel) suspended in 50 mM sodium citrate buffer (pH 4.8) as substrate. Reducing sugar release was quantified by the DNS method as described above. The 2.0 mL reaction mixture contained 0.5 mL of diluted crude enzyme and 1.5 mL substrate suspension, and was incubated at 50°C for 60 min in a shaking water bath to maintain uniform substrate dispersion. Subsequent color development and absorbance measurement were performed as described for endoglucanase.

2.3.7 *β*-Glucosidase activity

β-Glucosidase activity was determined using p-nitrophenyl-*β*-D-glucopyranoside (pNPG) as substrate. The 1.0 mL reaction system contained 50 mM sodium acetate buffer (pH 5.0), 1.0 mM pNPG, and 0.1 mL of diluted crude enzyme. After incubation at 50°C for 10 min, the reaction was terminated by adding 2.0 mL of 1.0 M Na_2CO_3, and absorbance was measured at 405 nm.

2.3.8 Filter paper activity (FPA)

Filter paper activity (representing total cellulolytic activity) was quantified by the DNS method as described above, using Whatman No. 1 filter paper as the standard substrate. A 60 mg filter paper strip (1 × 6 cm) was added to 1.5 mL of 50 mM sodium citrate buffer (pH 4.8). Reactions were initiated by adding 0.5 mL of diluted crude enzyme (total volume 2.0 mL) and incubated at 50°C for 60 min. Color development and absorbance measurement were performed as described for endoglucanase.

All enzyme assays were performed in triplicate, with heat-inactivated crude enzyme used as the blank control for each reaction. One unit (U) of enzyme activity was defined as the amount of enzyme that formed 1 μmol of the specified reaction product per minute under the assay conditions, and activities were expressed as U mL^{-1} of crude extract. Reducing sugars measured by the DNS assays were expressed as glucose equivalents, whereas *β*-glucosidase activity in the pNPG assay was based on p-nitrophenol formation.

2.4 Screening and validation of mycelial growth conditions

Culture conditions affecting the mycelial growth of *I. lacteus* n6 were first evaluated in single-factor experiments. The tested factors were temperature (10, 15, 20, 25, 30, 35, and 40°C), initial pH (4.5, 5.0, 5.5, 6.0, 6.5, 7.0, 7.5, and 8.0), carbon source (starch, maltose, glucose, fructose, sucrose, and lactose), and nitrogen source (peptone, aspartic acid, glutamic acid, and sodium nitrate). Based on the single-factor results, an $L_9(3^4)$ orthogonal design was used to screen carbon source, nitrogen source, initial pH, and temperature, each at three levels. Radial growth was measured daily, and colony morphology was recorded. The combination predicted by main-effect analysis was then compared experimentally with the best-performing orthogonal run using three independent biological replicates.

2.5 Screening of grain-based propagation media

Buckwheat, sorghum, maize, millet, and wheat were evaluated as grain-based media for the propagation of *I. lacteus* n6. Each medium contained 98% (w/w) of the corresponding grain, 1% (w/w) gypsum, and

1% (w/w) sucrose. The moisture content was adjusted to approximately 65%, after which the ingredients were thoroughly mixed, packed in heat-resistant polypropylene bags (17 × 33 cm), and autoclaved at 121°C for 20 min. After cooling, 30 g of each sterilized medium was aseptically transferred to a Petri dish and inoculated with n6. Ten independent replicate plates were prepared for each grain treatment. Colony diameter was monitored during incubation, and the mycelial growth rate (mm d^{-1}) was calculated to compare propagation among the five grain substrates.

2.6 Substrate pretreatment and SSF

To evaluate the effects of thermal pretreatment and inoculation with *I. lacteus* n6 on the composition of shredded *C. korshinskii* residues, the pretreatments were autoclaving at 121°C for 20 min and pasteurization at 80°C for 6 h, the substrates were either inoculated or left uninoculated. Each substrate was placed in a cylindrical culture vessel (10 cm in diameter and 15 cm in height). After cooling to room temperature, the inoculated groups received buckwheat grain spawn of n6 at 5% (w/w), whereas the corresponding controls remained uninoculated. The four treatments were autoclaved and uninoculated (AC−), autoclaved and inoculated (AC+), pasteurized and uninoculated (PA−), and pasteurized and inoculated (PA+). All substrates were incubated aerobically at 25°C for 56 d. Each treatment comprised three independent biological replicates.

2.7 Determination of nutritional composition and lignocellulosic fractions

After 56 d of incubation, substrate samples were predried at 65°C for 48 h and ground to pass through a 1-mm sieve. Dry matter (DM) content was determined on separate aliquots according to GB/T 6435 – 2014. Crude protein (CP) was determined by the Kjeldahl method using an automatic nitrogen analyzer according to GB/T 6432 – 2018. Ether extract (EE), crude ash, calcium (Ca), and phosphorus (P) were determined according to GB/T 6433 – 2006, GB/T 6438 – 2007, GB/T 6436 – 2018, and GB/T 6437 – 2018, respectively. Water-soluble carbohydrates (WSC) were extracted with water and quantified using the anthrone colorimetric method with glucose as the calibration standard. Neutral detergent fiber (NDF), acid detergent fiber (ADF), and acid detergent lignin (ADL) were determined according to Van Soest et al. (1991). Except for DM, all compositional data were expressed as percentages of DM.

2.8 Statistical analysis

Statistical analyses were performed using IBM SPSS 25.0 (IBM Corp., Armonk, NY, USA), and figures were prepared using GraphPad Prism 8.0 (GraphPad Software, La Jolla, CA, USA). Normality and homogeneity of variance were assessed using the Shapiro-Wilk and Levene tests, respectively. Differences among multiple treatments were evaluated by one-way analysis of variance followed by Tukey's honestly significant difference test. Colony diameter data were analyzed separately at each sampling time. The $L_9(3^4)$ experiment was evaluated by range analysis and a general linear model. In the validation experiment, the predicted combination was compared with the best-performing orthogonal-run combination using a two-sided independent-samples t-test. Statistical significance was set at $P < 0.05$.

3. Results and discussion

3.1 Antagonistic interactions among *I. lacteus* isolates

Pairwise confrontation assays revealed clear interaction zones between colonies of all eleven *I. lacteus* isolates (n1-n11) on PDA (Fig. 1A, Fig. S1). The width of the interaction zone and its internal mycelial density varied across pairwise strain combinations, ranging from narrow, faint contact interfaces to prominent, well-defined barrage lines, yet a distinct demarcation zone was detectable in all pairings (Fig. 1B, Fig. S1). In basidiomycetes, vegetative incompatibility is a self/non-self recognition response between genetically distinct conspecific mycelia. Such interactions restrict hyphal fusion and form distinct demarcation boundaries at colony interfaces (Worrall, 1997). Comparable demarcation lines accompanied by localized hyphal damage have been reported between incompatible isolates of *Helicobasidium mompa* (Inoue et al., 2011). The variation observed here indicates diversity in vegetative interaction phenotypes, although it does not by itself establish the genetic relationships among isolates.

3.2 Mycelial growth of *I. lacteus* isolates on *C. korshinskii* residue medium

Rapid substrate colonization is a critical trait for fungal performance in SSF and lignocellulosic biomass bioconversion, as it supports rapid establishment and competitive dominance on the substrate (Zhou et al., 2015). All eleven *I. lacteus* isolates grew progressively on shredded *C. korshinskii* residue medium during the 7-d observation period, but colony expansion differed significantly among isolates (Fig. 2A; Fig. S2). Isolates n4 and n6 reached the maximum measurable colony diameter of 70.00 mm and did not differ significantly from each other. Isolate n11 reached 66.39 mm, followed by n2 and n8, whereas n5 and n10 produced the smallest colonies and did not differ significantly from each other ($P > 0.05$; Fig. 2B).

Representative colony images agreed with the quantitative data. Isolates n4 and n6 formed dense white mycelia that extensively covered the substrate, whereas n5 and n10 showed weaker and less uniform colony development (Fig. 2C). The full time-course images further confirmed isolate-dependent differences in colonization rate and extent (Fig. S2). These results demonstrate marked intraspecific variation among *I. lacteus* isolates in their ability to colonize *C. korshinskii* residues. The rapid radial expansion and dense aerial mycelium exhibited by isolates n4 and n6 may reflect strain-specific adaptation to lignified shrub biomass, possibly mediated by coordinated oxidative and hydrolytic enzyme responses to lignocellulosic substrates (Qin et al., 2018).

3.3 Qualitative screening of the lignocellulose-degrading capacity

All eleven *I. lacteus* isolates formed reddish-brown oxidation zones on guaiacol-amended PDA, indicating their ability to oxidize this phenolic substrate, although the extent of oxidation varied markedly among

isolates (Fig. 3; Table S1). Guaiacol is structurally related to lignin-derived phenolic compounds and is widely used as an indicator substrate for preliminary screening of laccase-producing fungi, as its oxidation yields a characteristic visible reddish-brown product (Zhang et al., 2022). Isolate n11 produced the largest colony and oxidation zone. In contrast, n6 formed a relatively small colony (34.57 mm), but its oxidation zone reached 38.26 mm, resulting in the lowest colony-to-zone diameter ratio (R/r = 0.90; Fig. 3B). This ratio did not differ significantly from those of n3 and n9 ($P > 0.05$). Conversely, n7 and n10 presented the highest R/r ratios, at 1.67 and 1.45, respectively. As a lower R/r value corresponds to a larger oxidation zone relative to colony size, n6 displayed the strongest relative oxidative activity among the isolates tested. Guaiacol oxidation, however, can be mediated by laccase as well as other extracellular oxidoreductases. This assay should therefore be regarded as a qualitative or semiquantitative screen, and actual enzyme production by selected isolates requires further validation via quantitative activity assays (Kiiskinen et al., 2004).

All isolates decolorized aniline blue, suggesting potential extracellular ligninolytic activity, although the R/r values differed significantly among isolates (Fig. 3; Table S2). Aniline blue decolorization is commonly used as a preliminary indicator of LiP- and MnP-associated oxidative activity in ligninolytic microorganisms (Zhang et al., 2021). Isolate n5 produced the largest decolorized zone, followed by n6 and n1. Correspondingly, n5 and n6 exhibited the lowest R/r ratios, followed closely by n1, with no significant difference among the three isolates ($P > 0.05$). In contrast, n2 and n10 showed the highest ratios, indicating weaker decolorization relative to colony expansion. Thus, n5, n6, and n1 showed the strongest relative decolorization capacities. Because aniline blue can be degraded by several extracellular oxidative enzymes, these results should be interpreted as evidence of potential ligninolytic or peroxidase activity rather than as specific confirmation of LiP or MnP production (Zhang et al., 2021).

Congo red binds to undegraded β-1,4-D-glucan chains in CMC and gives the medium a red color. Fungal extracellular cellulases, particularly endoglucanases, hydrolyze the β-1,4-glycosidic bonds in CMC, reducing its ability to bind Congo red and producing clear or lightly colored hydrolysis zones around colonies. Hydrolysis zone formation can therefore be used as a qualitative indicator of extracellular cellulolytic activity (Florencio et al., 2012; Teather and Wood, 1982). Isolates n4 and n8 exhibited the lowest R/r values, both at 0.67, indicating the strongest relative CMC-hydrolyzing capacities (Fig. 3; Table S3). Isolates n2, n1, and n9 showed intermediate ratios of 0.82, 0.83, and 0.83, respectively, whereas n5 and n11 had the highest ratios, indicating comparatively limited hydrolysis relative to mycelial growth. The CMC-Congo red assay provides a rapid semiquantitative indication of extracellular cellulolytic potential, but it mainly reflects endoglucanase-mediated hydrolysis of soluble CMC and should not be interpreted as a direct quantitative measurement of total cellulase activity.

Taken together, the three plate assays revealed clear isolate-dependent differences in lignocellulose-degrading potential. Based on their performance in substrate colonization, guaiacol oxidation, aniline blue decolorization, and CMC hydrolysis, isolates n1, n6, n8 and n9 were selected for subsequent quantitative enzyme activity assays.

3.4 Lignocellulose-degrading enzyme activities of selected *I. lacteus* isolates

After 10 d of cultivation on shredded *C. korshinskii* residue medium, isolates, n1, n6, n8, and n9 showed distinct ligninolytic enzyme profiles (Fig. 4). Isolate n6 had the highest activities of MnP, LiP, and laccase, reaching 9.30, 11.33, and 3.59 U mL^{-1}, respectively, and each enzyme activity was significantly higher than the corresponding activity in the other isolates ($P < 0.05$). MnP activities were comparable in n1 and n8, while n9 had the lowest activity (Fig. 4A). LiP activities were intermediate and comparable in n8 and n9, whereas n1 had the lowest activity (Fig. 4B). Laccase showed a similar pattern, with the highest activity in n6 and the lowest in n9 (Fig. 4C). Thus, n6 had the strongest oxidative enzyme profile among the selected isolates.

The isolates also differed in cellulolytic enzyme activities (Fig. 5). Endoglucanase activity was highest in n8, followed by n6 and n1, and lowest in n9 (Fig. 5A). In contrast, n6 had the highest exoglucanase activity, reaching 17.53 U mL^{-1} and significantly exceeding that of the other isolates (Fig. 5B). *β*-Glucosidase activity was also highest in n6, although it did not differ significantly from that in n1, while n9 showed the lowest activity (Fig. 5C). Isolate n6 also had the highest FPA, reaching 13.88 U mL^{-1}, followed by n9, n8, and n1 (Fig. 5D). Although n6 did not have the highest endoglucanase activity, it combined strong exoglucanase, *β*-glucosidase, and total cellulase activities with the strongest ligninolytic profile.

The enzyme profile of n6 provides stronger evidence of its process suitability than the qualitative plate assays alone. LiP can oxidize high-redox-potential non-phenolic lignin structures, MnP generates diffusible Mn^{3+} chelates that attack phenolic lignin beyond the immediate hyphal surface, and laccase oxidizes phenolic lignin units, particularly in the presence of natural mediators. Concurrent production of these enzymes may broaden both the chemical range and spatial extent of oxidative modification within lignified shrub cell walls. Cellulolytic enzymes can then act on more accessible polysaccharides: endoglucanase cleaves internal cellulose chains, exoglucanase releases cellobiose from chain ends, and *β*-glucosidase converts cellobiose to glucose. Genomic and transcriptomic analyses similarly indicate that *I. lacteus* possesses an integrated oxidative–hydrolytic enzyme system and can induce manganese peroxidases before cellulases and hemicellulases accumulate (Qin et al., 2018). Enhanced sugar recovery has also been reported when ligninolytic enzymes from *I. lacteus* were combined with cellulases during wheat-straw hydrolysis (Salvachúa et al., 2013a). On this basis, n6 was selected as the optimal strain among the four quantitatively tested isolates for subsequent SSF and culture optimization experiments.

3.5 Evaluation and validation of culture conditions for *I. lacteus* n6

Temperature significantly affected the mycelial growth of *I. lacteus* n6 (Fig. 6A). The isolate grew from 10 to 40°C, with growth increasing to a maximum at 35°C and then declining at 40°C to approximately 64%

of the maximum. This pattern agrees with a reported optimum of 30–35°C for *I. lacteus* mycelial growth (Dong et al., 2017).

Initial pH also influenced mycelial growth. Isolate n6 grew across the tested pH range of 4.5-8.0, with the highest radial growth rate at pH 4.5, followed by pH 5.0 (Fig. 6B). Growth remained relatively high between pH 5.5 and 6.0 but declined as the medium became less acidic. Broad pH tolerance has also been reported for *I. lacteus* in submerged culture, with growth occurring between pH 3 and 9 (Dong et al., 2017). Reported pH optima vary among strains and enzyme systems: cellulase production by strain Il-11 was highest at initial pH of 4.0, whereas response-surface optimization of endoglucanase production by strain LBM 034 identified pH 5.5 as optimal (Giorgio et al., 2025).

The carbon source experiment showed that n6 could utilize several carbohydrate substrates, including monosaccharides, disaccharides, and starch (Fig. 6C). Glucose and maltose supported the highest growth rates, followed closely by starch. Fructose, sucrose, and lactose supported lower growth, and the control showed the weakest response. The favorable performance of starch is consistent with previous observations for *I. lacteus* growth (Dong et al., 2017), while its broad repertoire of carbohydrate-active enzymes may support growth on diverse carbohydrates (Qin et al., 2018).

Nitrogen source had a pronounced effect on n6 growth (Fig. 6D). Glutamic acid supported the highest radial growth rate, followed by aspartic acid. Peptone supported intermediate growth, whereas sodium nitrate and the control supported lower growth. Peptone has also been identified as an important medium component for cellulase production by *I. lacteus* (Giorgio et al., 2025).

The subsequent $L_9(3^4)$ orthogonal experiment evaluated the combined effects of carbon source, nitrogen source, initial pH, and temperature on n6 growth (Table 2). All four main effects were significant ($P < 0.001$). Based on the F values and ranges of the level means, temperature had the greatest effect, followed by nitrogen source, carbon source, and initial pH. Among the nine combinations, run 4 (maltose, peptone, initial pH of 5.0, and 35°C; $A_2B_1C_2D_3$) produced the highest observed growth rate of 18.05 ± 0.06 mm d^{-1} (Table 2a). Main-effect analysis predicted $A_2B_1C_1D_2$, corresponding to maltose, peptone, initial pH of 4.5, and 30°C, as the preferred combination within the tested levels (Table 2b). Interactions among the factors were not estimated independently in the $L_9(3^4)$ design. In the validation experiment, $A_2B_1C_1D_2$ produced a growth rate of 18.44 ± 0.32 mm d^{-1}, and no significant difference was detected relative to the best-performing orthogonal run ($P > 0.05$; Table 2c). Thus, maltose, peptone, an initial pH of 4.5, and 30°C were selected as suitable culture conditions for *I. lacteus* n6, providing a basis for inoculum preparation and subsequent SSF of *C. korshinskii* residues (Novotný et al., 2009; Rothschild et al., 2002).

Table 2. $L_9(3^4)$ orthogonal screening and validation of culture conditions for *I. lacteus* n6.

a Orthogonal design and observed growth rates

Run	A: Carbon source	B: Nitrogen source	C: Initial pH	D: Temperature (°C)	Growth rate (mm d^{-1})
1	Starch	Peptone	4.5	25	14.51 ± 0.46^{d}
2	Starch	Aspartic acid	5.0	30	16.25 ± 0.36^{bc}
3	Starch	Glutamic acid	5.5	35	14.63 ± 0.27^{d}
4	Maltose	Peptone	5.0	35	18.05 ± 0.06^{a}
5	Maltose	Aspartic acid	5.5	25	13.09 ± 0.30^{e}
6	Maltose	Glutamic acid	4.5	30	16.74 ± 0.45^{b}
7	Glucose	Peptone	5.5	30	16.13 ± 0.39^{bc}
8	Glucose	Aspartic acid	4.5	35	15.75 ± 0.41^{c}
9	Glucose	Glutamic acid	5.0	25	12.22 ± 0.16^{f}

b Main-effect and ANOVA results

Factor	k_1 (mm d^{-1})	k_2 (mm d^{-1})	k_3 (mm d^{-1})	R	F	P	Optimal level
Carbon source (A)	15.13	15.96	14.70	1.26	31.508	<0.001	A_2 (maltose)
Nitrogen source (B)	16.23	15.03	14.53	1.70	58.667	<0.001	B_1 (peptone)
Initial pH (C)	15.67	15.51	14.62	1.05	24.596	<0.001	C_1 (pH 4.5)
Temperature (D)	13.27	16.37	16.14	3.10	228.510	<0.001	D_2 (30 °C)

c Experimental validation of the culture-condition combination predicted by the main-effect analysis.

Treatment	Carbon source	Nitrogen source	Initial pH	Temperature (°C)	Growth rate (mm d^{-1})
Predicted combination ($A_2B_1C_1D_2$)	Maltose	Peptone	4.5	30	18.44 ± 0.32^{a}
Best observed run ($A_2B_1C_2D_3$)	Maltose	Peptone	5.0	35	18.05 ± 0.06^{a}

Growth rates are presented as means ± SD of three independent biological replicates. In section (a), different lowercase superscript letters indicate significant differences among experimental runs according to one-way ANOVA followed by Tukey's honestly significant difference test ($P < 0.05$). In section (b), k_1, k_2, and k_3 are the mean growth rates at levels 1, 2, and 3 of each factor, respectively, and R is the difference between the highest and lowest level means. For factor A, levels 1-3 represent starch, maltose, and glucose; for factor B, they represent peptone, aspartic acid, and glutamic acid; for factor C, they represent initial pH values of 4.5, 5.0, and 5.5; and for factor D, they represent 25, 30, and 35 °C. The F and *P* values test the four main effects. Interactions were aliased with the main effects and were not estimated independently in the $L_9(3^4)$ design. Main-effect analysis predicted $A_2B_1C_1D_2$ (maltose, peptone, initial pH of 4.5, and 30 °C) as the preferred combination within the tested levels. In section (c), this combination was compared experimentally with the best-performing orthogonal run, $A_2B_1C_2D_3$. No significant difference was detected between the two combinations using a two-sided independent-samples t-test ($P > 0.05$); this result should not be interpreted as statistical equivalence.

3.6 Screening of grain-based propagation media for *I. lacteus* n6

The *I. lacteus* n6 colonized all five tested grain substrates, but mycelial growth rates differed significantly among media (Fig. 7A). Buckwheat supported the highest growth rate (16.44 ± 0.40 mm d^{-1}), followed by sorghum (14.78 ± 0.42 mm d^{-1}), maize (12.65 ± 0.23 mm d^{-1}), millet (12.47 ± 0.33 mm d^{-1}), and wheat (12.13 ± 0.33 mm d^{-1}). Growth on buckwheat was significantly greater than that on all other substrates.

Colony morphology was consistent with the growth-rate data (Fig. 7B). Buckwheat supported dense, uniform white mycelium, and sorghum also allowed extensive colonization. Maize and millet supported intermediate colony development, whereas wheat showed comparatively weaker mycelial expansion. Inoculum-medium composition is known to affect fungal propagation. For example, one *I. lacteus* isolate fully colonized wheat grain spawn within 17 ± 2 d, compared with 27 ± 2 d on wheat grain supplemented with wood chips; liquid-medium screening also identified wheat thin stillage as a suitable substrate for pre-inoculum production (Salvachúa et al., 2013b; Shahtahmasebi et al., 2018). Buckwheat was therefore selected as the propagation medium for preparing n6 inoculum for subsequent fermentation of *C. korshinskii* residues.

3.7 Effects of thermal pretreatment and I. lacteus n6 inoculation on the composition of C. korshinskii residues

Microbial fermentation can modify the nutritional composition of agricultural and forestry residues and reduce recalcitrant lignocellulosic fractions, thereby supporting their potential use as feed. The lignocellulose-degrading capacity of *I. lacteus* has been reported during the treatment of corn stover (Xu et al., 2009), wheat straw (Chen et al., 2023), and buckwheat straw (Cao et al., 2023), whereas its application to *C. korshinskii* has rarely been examined. In this study, thermal pretreatment and

inoculation with *I. lacteus* n6 affected the chemical composition of shredded *C. korshinskii* residues after 56 d of incubation (Table 3). Significant pretreatment × inoculation interactions were detected for CP and WSC ($P < 0.001$ and $P = 0.017$, respectively). Under autoclaving, inoculation increased CP from 8.20% to 9.51% and WSC from 0.87% to 4.91%. Under pasteurization, the corresponding increases were from 8.18% to 12.10% and from 0.99% to 5.53%. The increases in CP were consistent with previous fungal-fermentation studies. For example, *Pleurotus ostreatus* fermentation increased the CP concentration of wheat straw from 3.37% to 5.08%, while *I. lacteus* treatment increased CP concentrations in corn stover and wheat straw (Shrivastava et al., 2011; Zuo et al., 2018). Inoculation also increased the concentrations of ash and phosphorus and decreased the calcium concentration under both pretreatments. A significant pretreatment × inoculation interaction was also detected for EE ($P = 0.028$): AC+ contained less EE than AC−, whereas no significant difference was detected between PA + and PA−.

Table 3
Chemical composition of *C. korshinskii* residues following thermal pretreatment and fungal inoculation.

Parameter	Autoclaving		Pasteurization		P		
(%DM)	AC−	AC+	PA−	PA+	P□	P_i	P□×$_i$
DM	91.53 ± 0.29^{d}	94.65 ± 0.41^{b}	92.75 ± 0.38^{c}	96.70 ± 0.35^{a}	< 0.001	< 0.001	0.081
CP	8.20 ± 0.10^{c}	9.51 ± 0.22^{b}	8.18 ± 0.25^{c}	12.10 ± 0.18^{a}	< 0.001	< 0.001	< 0.001
EE	3.80 ± 0.30^{a}	2.48 ± 0.25^{b}	3.71 ± 0.22^{a}	3.20 ± 0.27^{a}	0.071	< 0.001	0.028
Ash	3.16 ± 0.34^{b}	7.23 ± 0.38^{a}	3.26 ± 0.31^{b}	7.67 ± 0.29^{a}	0.196	< 0.001	0.401
Ca	1.51 ± 0.10^{a}	0.93 ± 0.07^{b}	1.49 ± 0.08^{a}	1.02 ± 0.09^{b}	0.500	< 0.001	0.299
P	0.09 ± 0.03^{b}	0.19 ± 0.02^{a}	0.11 ± 0.02^{b}	0.24 ± 0.02^{a}	0.029	< 0.001	0.290
WSC	0.87 ± 0.06^{c}	4.91 ± 0.19^{b}	0.99 ± 0.17^{c}	5.53 ± 0.12^{a}	0.002	< 0.001	0.017
NDF	72.37 ± 1.60^{a}	69.06 ± 1.18^{ab}	68.55 ± 1.04^{b}	57.05 ± 1.42^{c}	< 0.001	< 0.001	< 0.001
ADF	62.37 ± 1.36^{a}	58.01 ± 0.83^{b}	63.30 ± 0.76^{a}	52.83 ± 1.21c	0.009	< 0.001	0.001
ADL	14.97 ± 0.29^{b}	11.01 ± 0.27^{c}	16.08 ± 0.24^{a}	8.17 ± 0.31^{d}	< 0.001	< 0.001	< 0.001

Values are means ± SD of three independent biological replicates. DM is expressed as % of fresh mass; all other components are expressed as a % of DM. Different lowercase superscript letters within a row indicate significant pairwise differences among the four treatment means after Tukey adjustment ($P < 0.05$). P□, P_i, and P□×$_i$ are the P values for thermal pretreatment, inoculation, and their interaction, respectively, from two-way ANOVA. AC−, autoclaved and uninoculated; AC+, autoclaved and inoculated; PA−, pasteurized and uninoculated; PA+, pasteurized and inoculated. DM, dry matter; CP, crude protein; EE, ether extract; WSC, water-soluble carbohydrates; NDF, neutral detergent fiber; ADF, acid detergent fiber; ADL, acid detergent lignin; Ca, calcium; P, phosphorus.

Fiber fractions also showed significant pretreatment × inoculation interactions ($P < 0.001$; Table 3). Relative to PA−, PA + had 16.78% lower NDF, 16.54% lower ADF, and 49.19% lower ADL. Under autoclaving, inoculation reduced ADF and ADL by 6.99% and 26.45%, respectively. NDF was 4.57% lower in AC+ than in AC−, but the pairwise difference was not significant. These results indicate that pasteurization was associated with larger n6-related reductions in fiber and lignin concentrations than

autoclaving. The response is consistent with the broad set of carbohydrate-active and lignin-modifying enzymes reported for *I. lacteus* (Qin et al., 2018).

The stronger response following pasteurization agrees with reports that moderate thermal treatment can support *I. lacteus* colonization and lignocellulose conversion. Pasteurization at 80°C facilitated colonization of wheat straw and produced enzymatic sugar yields comparable to or greater than those obtained after autoclaving (Niu et al., 2023). Optimization of sterilization also enhanced delignification during *I. lacteus* fermentation of wheat straw (Zhu et al., 2024). Pasteurization at 70 or 80°C produced saccharification efficiencies comparable to or greater than autoclaving at 121°C for wheat and rapeseed straw, although autoclaving produced greater delignification of rice straw (Yuan et al., 2026).

One mechanistic explanation is that heating at 80°C sufficiently suppresses rapidly growing competitors to allow the inoculated n6 strain to establish on the substrate without complete sterilization. Similar hurdle strategies combining moderate heating, acidic conditions, or ensiling have improved the colonization of non-sterile lignocellulosic substrates by *I. lacteus* (Niu et al., 2020; Niu et al., 2023). From a feed perspective, reductions in NDF and ADF are potentially beneficial because high concentrations of these fractions can limit voluntary intake and ruminal digestibility (Nayan et al., 2019; Olagunju et al., 2024). The reduction in ADL is particularly relevant because lignin limits microbial access to structural polysaccharides and contributes to the formation of recalcitrant lignin-carbohydrate complexes (Nayan et al., 2020).

4. Conclusions

Sequential screening of eleven wild *I. lacteus* isolates identified isolate n6 as a locally derived strain with rapid colonization of *C. korshinskii* residues and a complementary ligninolytic and cellulolytic enzyme profile. Maltose, peptone, initial pH of 4.5, and 30°C supported mycelial growth, while buckwheat was the most suitable grain substrate among those tested for inoculum propagation. Compared with the uninoculated pasteurized control, pasteurization-assisted SSF with n6 reduced NDF, ADF, and ADL concentrations by 16.78%, 16.54%, and 49.19%, respectively. The measured CP and WSC concentrations also increased after fermentation. These findings demonstrate the feasibility of pasteurization-assisted solid-state bioconversion of *C. korshinskii* residues by *I. lacteus* n6 and support their potential for forage-oriented valorization. Further studies should evaluate digestibility, microbial stability and safety, and animal performance before practical feed applications can be established.

Declarations

Ethics approval and consent to participate

Not applicable.

Consent for publication

Not applicable.

Availability of data and material

The dataset(s) supporting the conclusions of this article are included within the article and its additional file(s). Additional raw data are available from the corresponding author upon reasonable request.

Competing interests

The authors declare no competing financial or non-financial interests.

Funding

This work was supported by the Inner Mongolia Autonomous Region Natural Science Foundation, China [grant number 2026MA0759]; and the Inner Mongolia Agricultural University [grant numbers XLY2025-2, LX20250625-7].

Authors' contributions

Xueying Liu: Methodology, Investigation, Funding acquisition. Liqiong Yan: Writing – original draft, Visualization, Data curation. Liyan Zhang: Investigation, Validation. Yaoran Zhang: Investigation, Formal analysis. Junhan Weng: Resources, Conceptualization. Yue Bai: Writing - review & editing, Methodology. Yanhong He: Writing - review & editing, Funding acquisition.

Acknowledgements

Not applicable.

References

1. Cao X, Zuo S, Cai R, Yang F, Jiang X, Xu C (2023) Expansion combined with Irpex lacteus fungal treatment for enhancing buckwheat straw degradation. Biochem Eng J 197:108994. https://doi.org/10.1016/j.bej.2023.108994
2. Chen H, Liang X, Li S, Cui Z, Yong Y, Ni Z, Bu Q, Zhu D (2023) Straw lignin degradation by lignin peroxidase from *Irpex lacteus* cooperated with enzymes and small molecules. Biotechnol Lett 45:95–104. https://doi.org/10.1007/s10529-022-03325-z
3. Dong X, Song X, Dong C (2017) Nutritional requirements for mycelial growth of milk-white toothed mushroom, *Irpex lacteus* (Agaricomycetes), in submerged culture. Int J Med Mushrooms 19:829–838. https://doi.org/10.1615/IntJMedMushrooms.2017 024530
4. Fang X, Li J, Xiong Y, Xu D, Fan X, Li F (2008) Responses of *Caragana korshinskii* Kom. to shoot removal: mechanisms underlying regrowth. Ecol Res 23:863–871. https://doi.org/10.1007/s11284-007-0449-x

5. Florencio C, Couri S, Farinas CS (2012) Correlation between agar plate screening and solid-state fermentation for the prediction of cellulase production by Trichoderma strains. Enzyme Res 2012:793708. https://doi.org/10.1155/2012/793708
6. Ghose TK (1987). Measurement of cellulase activities. Pure Appl Chem 59:257–268. http://dx.doi.org/10.1351/pac198759020257
7. Giorgio EM, Díaz GV, Saparrat MCN, Zapata PD (2025) Lignocellulosic bioconversion by an optimized enzymatic cocktail from *Irpex lacteus*. Asian J Mycol 8:76–91. https://doi.org/10.5943/ajom/8/2/6
8. Inoue K, Kanematsu S, Park P, Ikeda K (2011) Cytological analysis of mycelial incompatibility in *Helicobasidium mompa*. FEMS Microbiol Lett 315:94–100. https://doi.org/10.1111/j.1574-6968.2010.02174.x
9. Ju J, Zhang G, Xiao M, Dong C, Zhang R, Du L, Zheng Y, Wei M, Wei M, Wu B (2023) Effects of cellulase and Lactiplantibacillus plantarum on the fermentation quality, microbial diversity, gene function prediction, and in vitro rumen fermentation parameters of *Caragana korshinskii* silage. Front Food Sci Technol 2:1108043. https://doi.org/10.3389/frfst.2022.1108043
10. Kiiskinen LL, Rättö M, Kruus K (2004) Screening for novel laccase-producing microbes. J Appl Microbiol 97:640–646. https://doi.org/10.1111/j.1365-2672.2004.02348.x
11. Li SF, Wang H, Chen JL, Zhu HX, Yao RS, Wu H (2020) Degradation and transformation of lignin by a fungus Aspergillus flavus strain F-1. Iran J Biotechnol 18:e2461. https://doi.org/10.30498/IJB.2020.155690.2461
12. Li W, Zhang S, Zhang T, Shen Y, Han L, Peng Z, Xie Z, Zhong C, Jia S (2021) Bacterial cellulose production from ethylenediamine-pretreated *Caragana korshinskii* Kom. Ind Crops Prod 164:113340. https://doi.org/10.1016/j.indcrop.2021.113340
13. Liu Z, Fu T, Hu C, Shen D, Macchioni N, Sozzi L, Chen Y, Liu J, Tian X, Ge Q, Feng Z, Liu H, Zhang Z, Pan J (2018) Microbial community analysis and biodeterioration of waterlogged archaeological wood from the Nanhai No. 1 shipwreck during storage. Sci Rep 8:7170. https://doi.org/10.1038/s41598-018-25484-8
14. Ma W, Yan M, Zuo H, Chen X (2026) Regulatory effects of stubble management on leaf-soil carbon, nitrogen, and phosphorus stoichiometric relationships in *Caragana korshinskii.* Plants 15:1584. https://doi.org/10.3390/plants15101584
15. Makkar HPS (2018) Review: feed demand landscape and implications of food-not-feed strategy for food security and climate change. Animal 12:1744–1754. https://doi.org/10.1017/S175173111700324X
16. Mei F, Yang T, Chao H, Ma X, Wu J, Yang Q, Ren G, Song L, Wang Q, Qi L, Fu X, Gao C, Wang R, Chen M, Fang X, Liu J, Li G, Wu S (2025) Genomic insights into drought adaptation of the forage shrub *Caragana korshinskii* (Fabaceae) widely planted in drylands. Plant J 121:e17255. https://doi.org/10.1111/tpj.17255

17. Miller GL (1959). Use of dinitrosalicylic acid reagent for determination of reducing sugar. Anal Chem 31:426–428. https://doi.org/10.1021/ac60147a030
18. Nayan N, van Erven G, Kabel MA, Sonnenberg ASM, Hendriks WH, Cone JW (2019) Evaluation of fungal degradation of wheat straw cell wall using different analytical methods from a ruminant nutrition perspective. J Sci Food Agric 99:4054–4062. https://doi.org/10.1002/jsfa.9634
19. Nayan N, Sonnenberg ASM, Hendriks WH, Cone JW (2020) Prospects and feasibility of fungal pretreatment of agricultural biomass for ruminant feeding. Anim Feed Sci Technol 268:114577. https://doi.org/10.1016/j.anifeedsci.2020.114577
20. Niu D, Zuo S, Ren J, Huhetaoli, Zheng M, Jiang D, Xu C (2020) Novel strategy to improve the colonizing ability of *Irpex lacteus* in non-sterile wheat straw for enhanced rumen and enzymatic digestibility. Appl Microbiol Biotechnol 104:1347–1355. https://doi.org/10.1007/s00253-019-10315-1
21. Niu D, An W, Yu C, Zhu P, Li C, Yin D, Zhi J, Jiang X, Ren J (2023) Pre-pasteurization enhances the fermentation of wheat straw by *Irpex lacteus*: chemical composition, enzymatic hydrolysis, and microbial community. Ind Crops Prod 202:116962. https://doi.org/10.1016/j.indcrop.2023.116962
22. Novotný C, Cajthaml T, Svobodová K, Šusla M, Šašek V (2009) *Irpex lacteus*, a white-rot fungus with biotechnological potential—review. Folia Microbiol 54:375–390. https://doi.org/10.1007/s12223-009-0053-2
23. Olagunju LK, Isikhuemhen OS, Dele PA, Anike FN, Alabi JO, Ike KA, Shaw Y, Brice RM, Orimaye OE, Wuaku M, Udombang NS, Anele UY (2024) The impact of three white-rot fungi on nutrient availability, greenhouse gas emissions, and volatile fatty acid production in myceliated sorghum. Foods 13:2199. https://doi.org/10.3390/foods13142199
24. Qin X, Su X, Luo H, Ma R, Yao B, Ma F (2018) Deciphering lignocellulose deconstruction by the white-rot fungus *Irpex lacteus* based on genomic and transcriptomic analyses. Biotechnol Biofuels 11:58. https://doi.org/10.1186/s13068-018-1060-9
25. Rothschild N, Novotný Č, Šašek V, Dosoretz CG (2002) Ligninolytic enzymes of the fungus *Irpex lacteus* (Polyporus tulipiferae): isolation and characterization of lignin peroxidase. Enzyme Microb Technol 31:627–633. https://doi.org/10.1016/S0141-0229(02)00171-0
26. Rouches E, Zhou S, Steyer JP, Carrère H (2016) White-rot fungi pretreatment of lignocellulosic biomass for anaerobic digestion: impact of glucose supplementation. Process Biochem 51:1784–1792. https://doi.org/10.1016/j.procbio.2016.02.003
27. Salvachúa D, Martínez AT, Tien M, López-Lucendo MF, García F, de los Ríos V, Martínez MJ, Prieto A (2013a) Differential proteomic analysis of the secretome of *Irpex lacteus* and other white-rot fungi during wheat straw pretreatment. Biotechnol Biofuels 6:115. https://doi.org/10.1186/1754-6834-6-115
28. Salvachúa D, Prieto A, Vaquero ME, Martínez AT, Martínez MJ (2013b) Sugar recoveries from wheat straw following treatments with the fungus *Irpex lacteus*. Bioresour Technol 131:218–225. https://doi.org/10.1016/j.biortech.2012.11.089

29. Shahtahmasebi SH, Pourianfar HR, Mahdizadeh V, Shahzadeh Fazeli SA, Amoozegar MA, Nasr SH, Zabihi SS, Rezaeian SH, Malekzadeh KH, Janpoor J (2018) A preliminary study on domestication of wild-growing medicinal mushrooms collected from northern Iran. Curr Res Environ Appl Mycol 8:606–623. https://doi.org/10.5943/cream/8/6/4
30. Shrivastava B, Thakur S, Khasa YP, Gupte A, Puniya AK, Kuhad RC (2011) White-rot fungal conversion of wheat straw to energy-rich cattle feed. Biodegradation 22:823–831. https://doi.org/10.1007/s10532-010-9408-2
31. Teather RM, Wood PJ (1982) Use of Congo red–polysaccharide interactions in enumeration and characterization of cellulolytic bacteria from the bovine rumen. Appl Environ Microbiol 43:777–780. https://doi.org/10.1128/aem.43.4.777-780.1982
32. Tien M, Kirk TK (1988). Lignin peroxidase of *Phanerochaete chrysosporium*. Methods Enzymol 161:238–249. https://doi.org/10.1016/0076-6879(88)61025-1
33. Van Soest PJ, Robertson JB, Lewis BA (1991) Methods for dietary fiber, neutral detergent fiber, and nonstarch polysaccharides in relation to animal nutrition. J Dairy Sci 74:3583–3597. https://doi.org/10.3168/jds.S0022-0302(91)78551-2
34. Wang Y, Duan Y, Zhang M, Liang C, Li W, Liu C, Ye Y (2024) Genome sequencing and metabolic potential analysis of *Irpex lacteus*. J Fungi 10:846. https://doi.org/10.3390/jof10120846
35. Wariishi H, Valli K, Gold MH (1992). Manganese(II) oxidation by manganese peroxidase from the basidiomycete *Phanerochaete chrysosporium*. Kinetic mechanism and role of chelators. J Biol Chem 267:23688–23695. https://doi.org/10.1016/S0021-9258(18)35893-9
36. Worrall JJ (1997) Somatic incompatibility in basidiomycetes. Mycologia 89:24–36. https://doi.org/10.1080/00275514.1997.12026751
37. Xu C, Ma F, Zhang X (2009) Lignocellulose degradation and enzyme production by *Irpex lacteus* CD2 during solid-state fermentation of corn stover. J Biosci Bioeng 108:372–375. https://doi.org/10.1016/j.jbiosc.2009.04.023
38. Yu S, Yang J, Norghauer JM, Yang J, Yang B, Zhang H, Li X (2026) Water-use efficiency and plant–soil C:N:P stoichiometry in response to stand quality of *Caragana korshinskii* in the Mu Us Desert of China. Land Degrad Dev 37:5333–5344. https://doi.org/10.1002/ldr.70455
39. Yuan R, Wu Q, Li J, Niu D, Lei T, Huhe T (2026) Sterilization strategy determines degradation efficacy of diverse lignocellulosic biomasses by *Irpex lacteus*. Bioprocess Biosyst Eng 49:571–582. https://doi.org/10.1007/s00449-025-03274-7
40. Zhang Y, Wang M, Usman S, Li F, Bai J, Zhang J, Guo X (2023) Lignocellulose conversion of ensiled *Caragana korshinskii* Kom. facilitated by Pediococcus acidilactici and cellulases. Microb Biotechnol 16:432–447. https://doi.org/10.1111/1751-7915.14130
41. Zhang Z, Shah AM, Mohamed H, Tsiklauri N, Song Y (2021) Isolation and screening of microorganisms for the effective pretreatment of lignocellulosic agricultural wastes. Biomed Res Int 2021:5514745. https://doi.org/10.1155/2021/5514745

42. Zhang Z, Shah AM, Mohamed H, Zhang Y, Sadaqat B, Tsiklauri N, Sadunishvili T, Song Y (2022) Improved laccase production in Pleurotus djamor RP by atmospheric and room temperature plasma (ARTP) mutagenesis. Electron J Biotechnol 58:1–9. https://doi.org/10.1016/j.ejbt.2022.03.005
43. Zhou S, Raouche S, Grisel S, Navarro D, Sigoillot JC, Herpoël-Gimbert I (2015) Solid-state fermentation in multi-well plates to assess pretreatment efficiency of rot fungi on lignocellulose biomass. Microb Biotechnol 8:940–949. https://doi.org/10.1111/1751-7915.12307
44. Zhou T, Lei X, Luo Y, Ou Y, Tian S, Xie Y, Zheng Y, Sun H, Yang F (2025) High temperatures and antibacterial plant additives change the fermentation quality, free amino acids, and lactic acid bacteria fermentation type in *Caragana korshinskii* silage. BMC Microbiol 25:437. https://doi.org/10.1186/s12866-025-04153-7
45. Zhu P, Niu D, Zhang S, Li C, Yin D, Zhi J, Zhang L, Jiang X, Ren J (2024) Enhanced delignification and production of bioactive compounds in wheat straw by optimizing sterilization methods for *Irpex lacteus* fermentation. Food Chem 435:137570. https://doi.org/10.1016/j.foodchem.2023.137570
46. Zuo S, Niu D, Zheng M, Jiang D, Tian P, Li R, Xu C (2018) Effect of Irpex lacteus, Pleurotus ostreatus, and Pleurotus cystidiosus pretreatment of corn stover on its improvement of the in vitro rumen fermentation. J Sci Food Agric 98:4287–4295. https://doi.org/10.1002/jsfa.8951

Figures

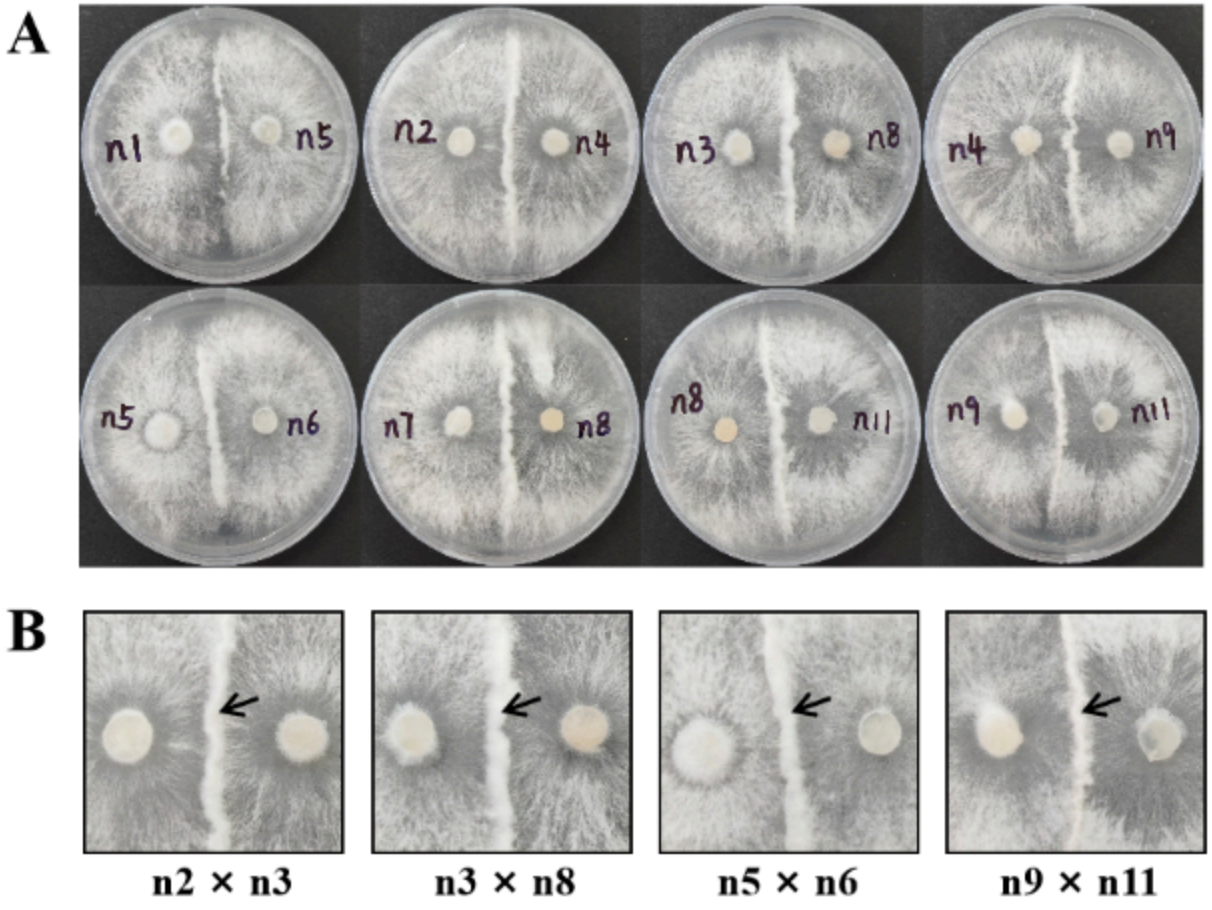


Figure 1

Representative pairwise mycelial interactions in *I. lacteus* isolates on PDA.

(A) Representative dual-culture pairings showing variation in the macroscopic interaction boundaries formed between isolates n1-n11. (B) Enlarged views of colony interfaces; arrows indicate visible demarcation or barrage lines.

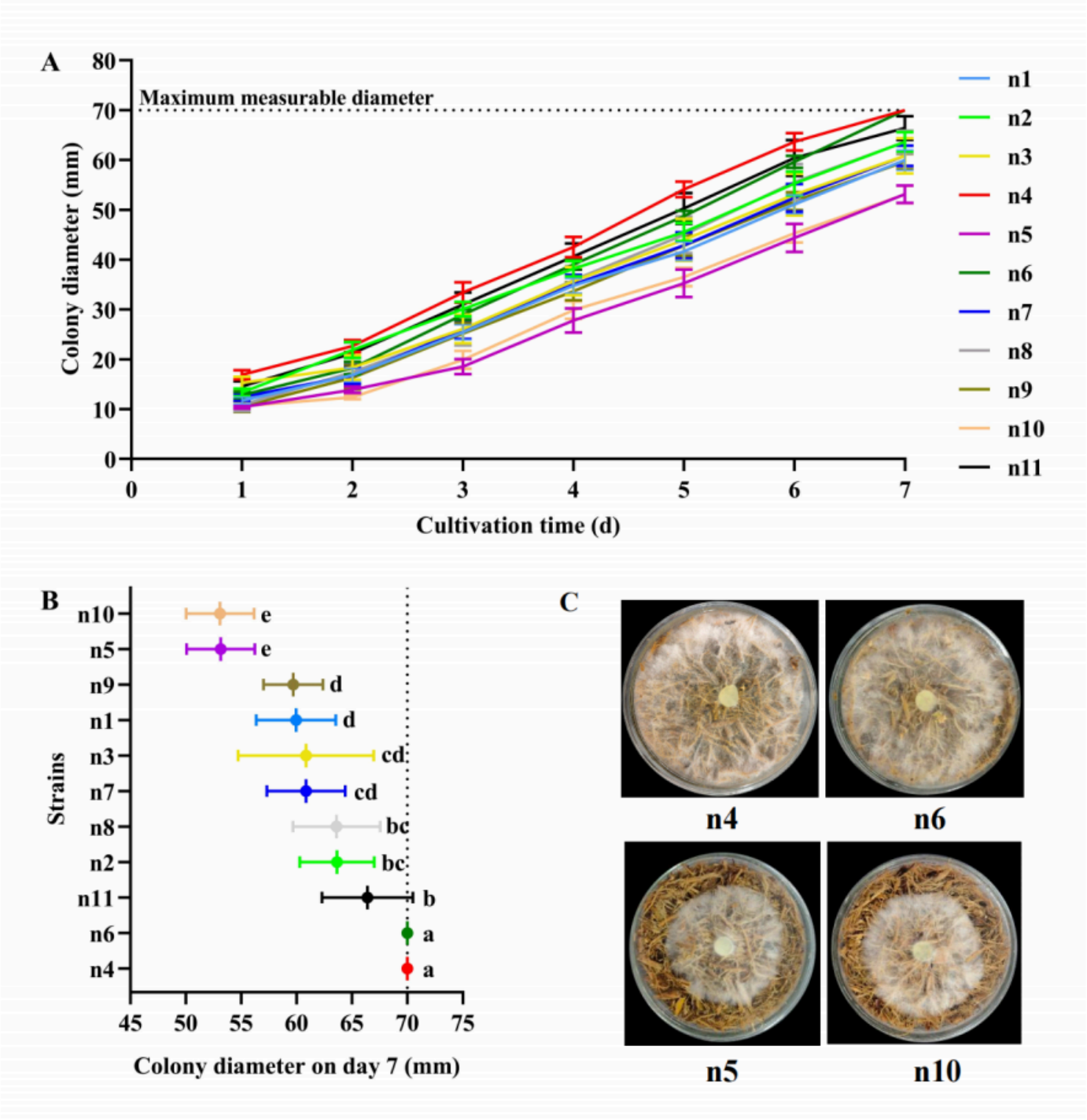


Figure 2

Growth and morphology of *I. lacteus* isolates on *C. korshinskii* residue.

(A) Changes in colony diameter during 7 d of cultivation. (B) Colony diameters on day 7. Points and horizontal error bars represent means ± SD of three independent biological replicates. Different lowercase letters indicate significant differences among isolates according to one-way ANOVA followed by Tukey's honestly significant difference test ($P < 0.05$). The reference lines in (A) and (B) indicate the maximum measurable colony diameter of 70 mm. (C) Representative colony morphology of isolates n4, n6, n5, and n10 on day 7.

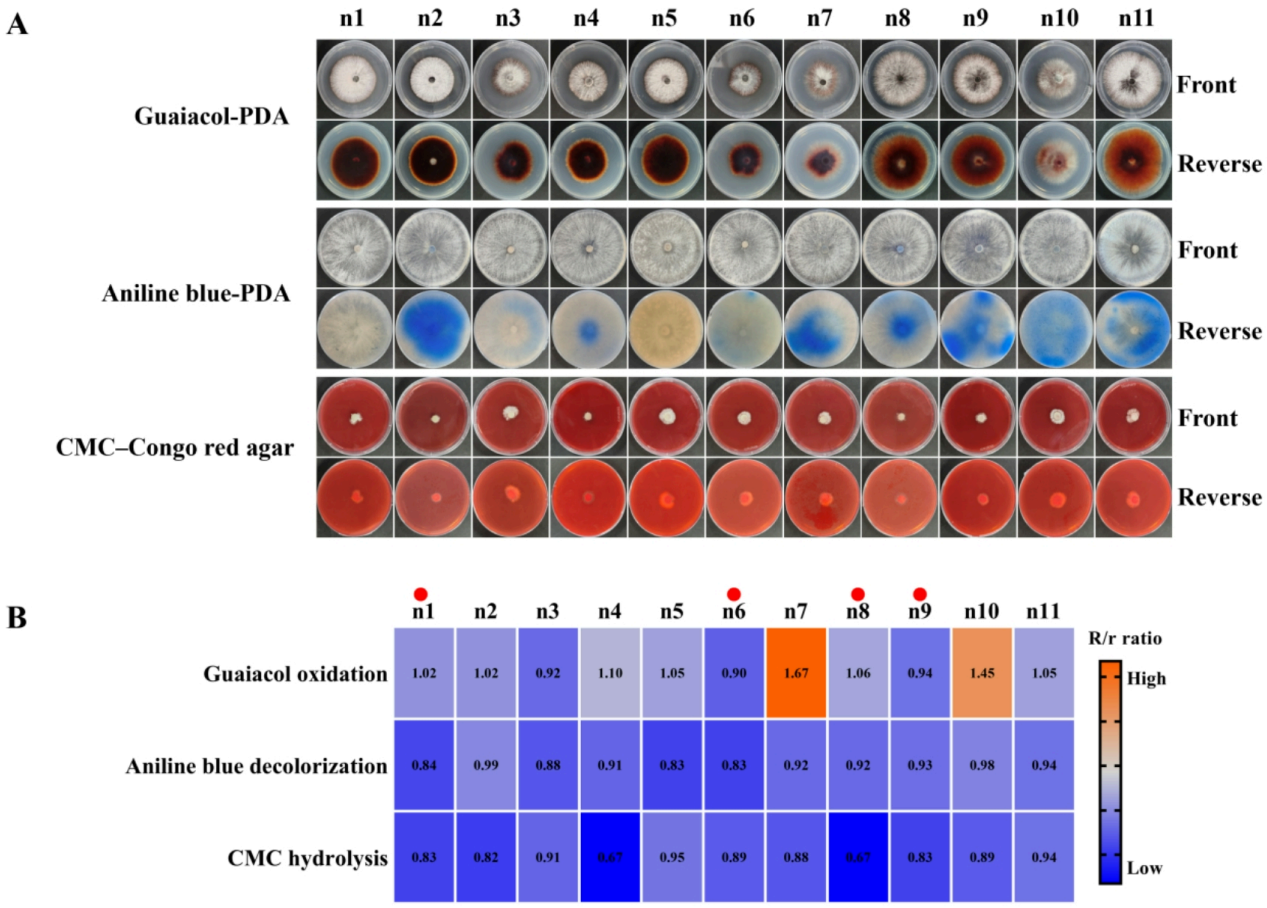


Figure 3

Qualitative plate screening of lignocellulose-degrading potential among *I. lacteus* isolates.

(A) Guaiacol oxidation, aniline blue decolorization, and carboxymethyl cellulose (CMC)-Congo red hydrolysis by 11 *I. lacteus* isolates. For each assay, the upper and lower rows show the front and reverse

sides of the cultures, respectively. (B) Heatmap of the colony-to-reaction-zone diameter ratio (R/r) for the guaiacol, aniline blue, and CMC-Congo red assays, shown from top to bottom. R and r denote the colony and reaction-zone diameters, respectively. Lower R/r values indicate larger reaction zones relative to colony size and therefore stronger relative oxidation, decolorization, or hydrolysis responses. The color scale ranges from blue for lower ratios to orange for higher ratios. Red circles identify isolates n1, n6, n8, and n9, which were selected for quantitative enzyme activity assays.

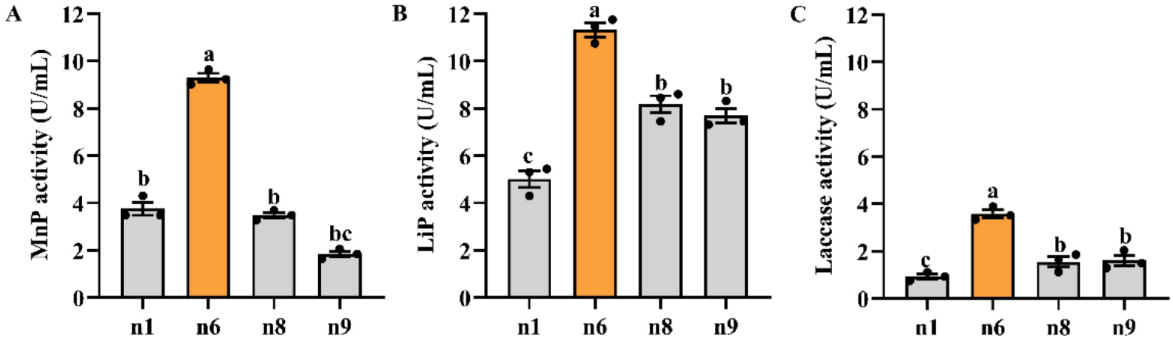


Figure 4

Ligninolytic enzyme activities of selected *I. lacteus* isolates.

Activities of manganese peroxidase (MnP; A), lignin peroxidase (LiP; B), and laccase (C) in isolates n1, n6, n8, and n9 after 10 d of cultivation. Bars and error bars represent means ± SD of three independent biological replicates, and dots indicate individual replicate values. Isolate n6 is highlighted in orange, and the other isolates are shown in gray. Different lowercase letters indicate significant differences among isolates within the same enzyme assay according to one-way ANOVA followed by Tukey's honestly significant difference test ($P < 0.05$).

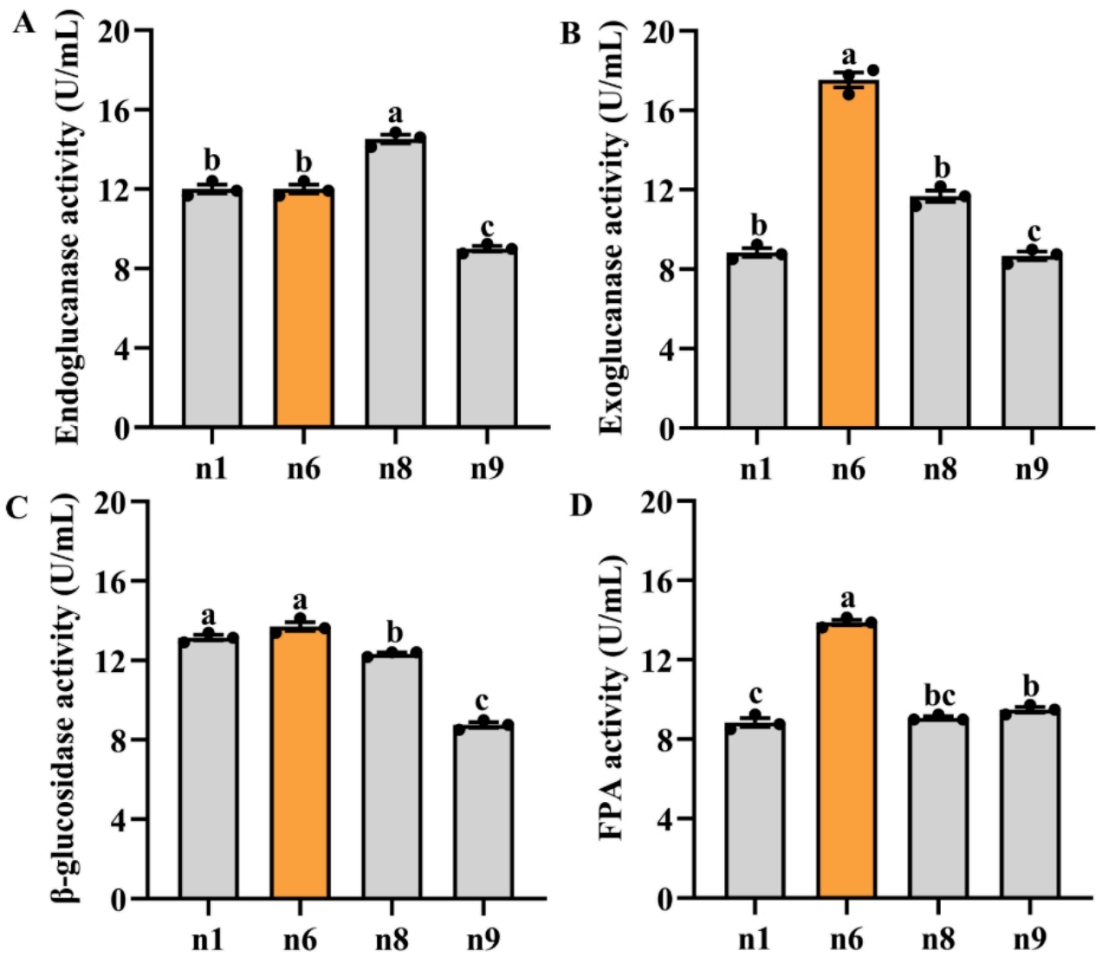


Figure 5

Cellulolytic enzyme activities of selected *I. lacteus* isolates.

Activities of endoglucanase (A), exoglucanase (B), *β*-glucosidase (C), and filter paper activity (FPA; D) in isolates n1, n6, n8, and n9 after 10 d of cultivation. Bars and error bars represent means ± SD of three independent biological replicates, and dots indicate individual replicate values. Isolate n6 is highlighted in orange, and the other isolates are shown in gray. Different lowercase letters indicate significant differences among isolates within the same enzyme assay according to one-way ANOVA followed by Tukey's honestly significant difference test ($P < 0.05$).

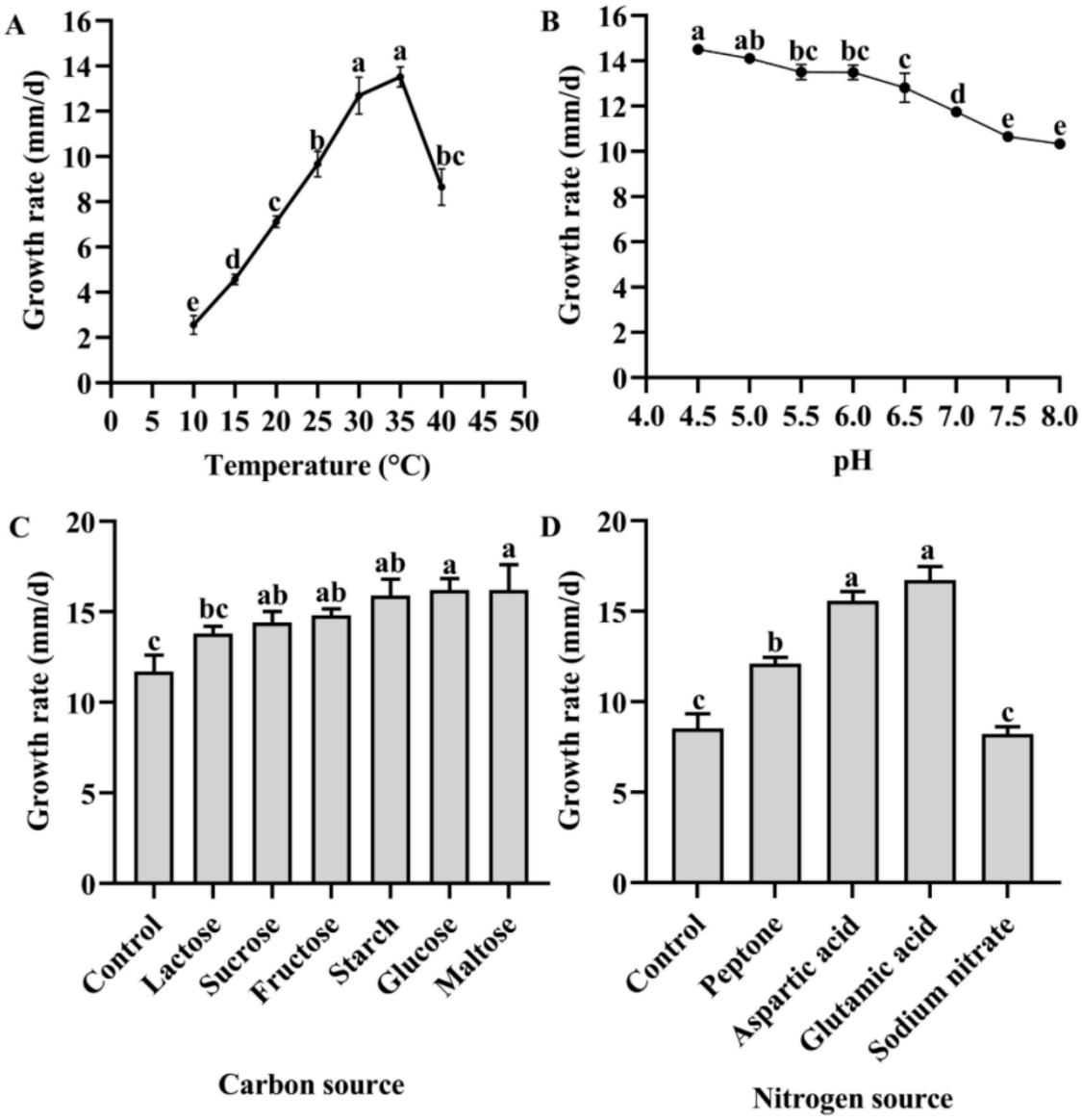


Figure 6

Effects of culture conditions on*l. lacteus* n6 growth.

Radial growth rates under different incubation temperatures (A), initial pH values (B), carbon sources (C), and nitrogen sources (D). Bars and error bars represent means ± SD of three independent biological replicates. Different lowercase letters indicate significant differences among treatments within each experiment according to one-way ANOVA followed by Tukey's honestly significant difference test ($P < 0.05$).

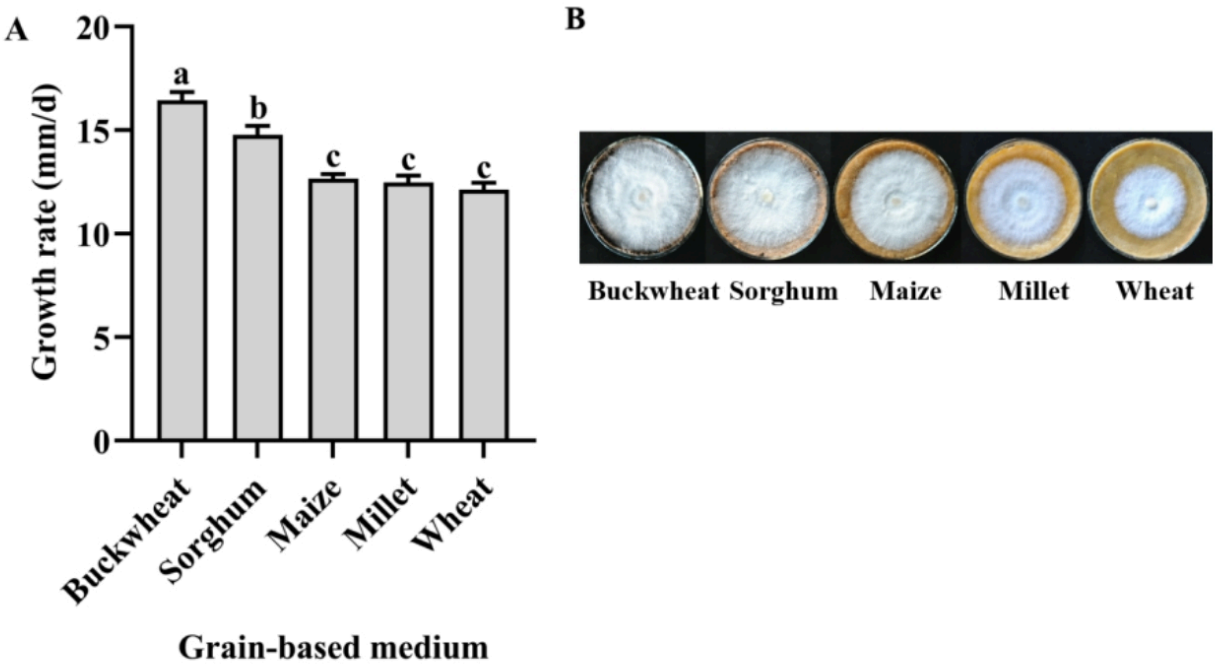


Figure 7

Screening of grain-based propagation media for *I. lacteus* n6.

(A) Colony-diameter growth rates on buckwheat, sorghum, maize, millet, and wheat media. Bars and error bars represent means ± SD of ten independent Petri-dish cultures per medium. Different lowercase letters indicate significant differences among grain-based media according to one-way ANOVA followed by Tukey's honestly significant difference test ($P < 0.05$). (B) Representative colony morphology of n6 on different grain-based media.

Supplementary Files

This is a list of supplementary files associated with this preprint. Click to download.

- FigsS1S2.docx
- GraphicalAbstract.png
- Supplementarymaterial.docx